

Supplementary materials

Site-specific recognition of Cov-SARS-2 nsp1 protein with a tailored titanium dioxide nanoparticle – elucidation of the complex structure using NMR data and theoretical calculation

P. Agback,^{a*} T. Agback,^a F. Dominguez,^b E.I. Frolova,^b G. Seisenbaeva,^a V. Kessler^{a*}

^a Department of Molecular Sciences, BioCenter, Swedish University of Agricultural Sciences, Box 7015, SE-75007, Uppsala, Sweden

^b Department of Microbiology, University of Alabama at Birmingham, 1720 2nd Ave South
Birmingham, AL 35294, USA

Materials and methods

As model for surface binding was chosen the structurally characterized and chemically individual spherical particle reported in 1.55 nm in geometric diameter³⁷.

$[(\text{NH}_4)_2\text{Ti}(\text{OCOCHOCH}_3)_3]_2 \cdot \text{EtOH}$ (**1**). Mother liquor after sedimentation of lactate-modified TiO_2 particles by addition of equal amount of 96% ethanol to 50 wt% solution of TiBALDH in water was left for drying in air, producing the rod-shaped crystals of **1**.

Characterization. TiO_2 content of the triethanolamine-derived sols was determined with PerkinElmer Pyris 1 thermobalance.

Crystallography. The data collection has been carried out at room temperature ($23 \pm 2^\circ\text{C}$) using Bruker D8 SMART Apex2 CCD diffractometer with MoK_α radiation ($\lambda = 0.7083 \text{ \AA}$) in the 2θ range $6.28 - 50.04^\circ$. $\text{C}_{20}\text{H}_{50}\text{N}_4\text{O}_{15}\text{Ti}_2$, $M = 682.44 \text{ Da}$, Monoclinic, Space Group C2, $a = 15.053(9)$, $b = 8.727(5)$, $c = 25.957(15) \text{ \AA}$, $\beta = 91.475(10)^\circ$, $V = 3409(3) \text{ \AA}^3$, $d_{\text{calc}} = 1.330 \text{ g/cm}^3$. 5760 symmetrically independent reflections with $R_{\text{int}} = 0.0346$ were obtained from data integration. The structure was solved by direct methods. The coordinates of all non-hydrogen were obtained from the initial solution and refined in isotropic and then anisotropic approximation. The hydrogen atoms were added by geometrical calculation for C-atoms and by differential Fourier syntheses for N-atoms and refined isotropically using a riding model. Final discrepancy values were $R1 = 0.0362$, $wR2 = 0.0833$ for 5098 reflections with $I > 2\sigma(I)$. Full details of structure solution and refinement are available free-of-charge from the Cambridge Crystallographic Data Centre citing the reference number **2086690**, at <https://www.ccdc.cam.ac.uk/solutions/csd-core/components/csd/>.

Protein expression and purification. The protein was prepared as described in reference 25.

NMR samples preparation. All NMR experiments were performed in a buffer containing 20 mM HEPES pH 7.5, 1 mM NaN_3 , 10 (v/v) % D_2O and 0.1 mM DSS (4,4-dimethyl-4-silapentane-1-sulfonic acid) as an internal ^1H chemical shift standard. Two such samples were prepared. The protein concentration was 0.25 mM, and all spectra were acquired in 3 mm tubes (final volume of 0.2 mL). ^{13}C and ^{15}N chemical shifts were referenced indirectly to the ^1H standard using a conversion factor derived from the ratio of NMR frequencies. The nanoparticles, NP1 and NP2, were dissolved in H_2O for a concentration of 500 mM and 50 mM, respectively.

NMR experiments. NMR experiments were acquired on Bruker Avance III spectrometers operating at 14.1 T, equipped with a cryo-enhanced QCI-P probe. All ^1H - ^{15}N TROSY experiments were run with 400 increments and 16 scans. As the first step we recorded TROSY spectra for the protein without anything added. Then we added 1 μL of the respective NP solution to form 1:1 complexes (NP1 solution was diluted 10 times with D₂O before) and TROSY was ran again. In a final step, 1 μL of NP1 was added to its 1:1 complex to change it into 10:1 and 1 μL of NP2 to its 1:1 complex to increase it to 2:1. Again TROSY spectra were recorded.

Modelling. Molecular graphics and analyses was performed with UCSF Chimera, developed by the Resource for Biocomputing, Visualization, and Informatics at the University of California, San Francisco, with support from NIH P41-GM103311. The 7K7P pdb file as well as a pdb file for the nanoparticle obtained from a cif file of the $\text{H}_6[\text{Ti}_{42}(\mu_3\text{-O})_{60}(\text{O}^i\text{Pr})_{42}(\text{OH})_{12}]$ structure was combined in chimera 1.15 and docking could be obtained by matching the sidechains of the amino acids showing chemical shift perturbation with the surface of the nanoparticle³⁸.

Description of NP1 material (reproduced with permission from Seisenbaeva G.A., Daniel G., Nedelec J.M., Kessler V.G., *Solution equilibrium behind room temperature synthesis of nanocrystalline titanium dioxide*, *Nanoscale* 2013, 5, 3330-3336)

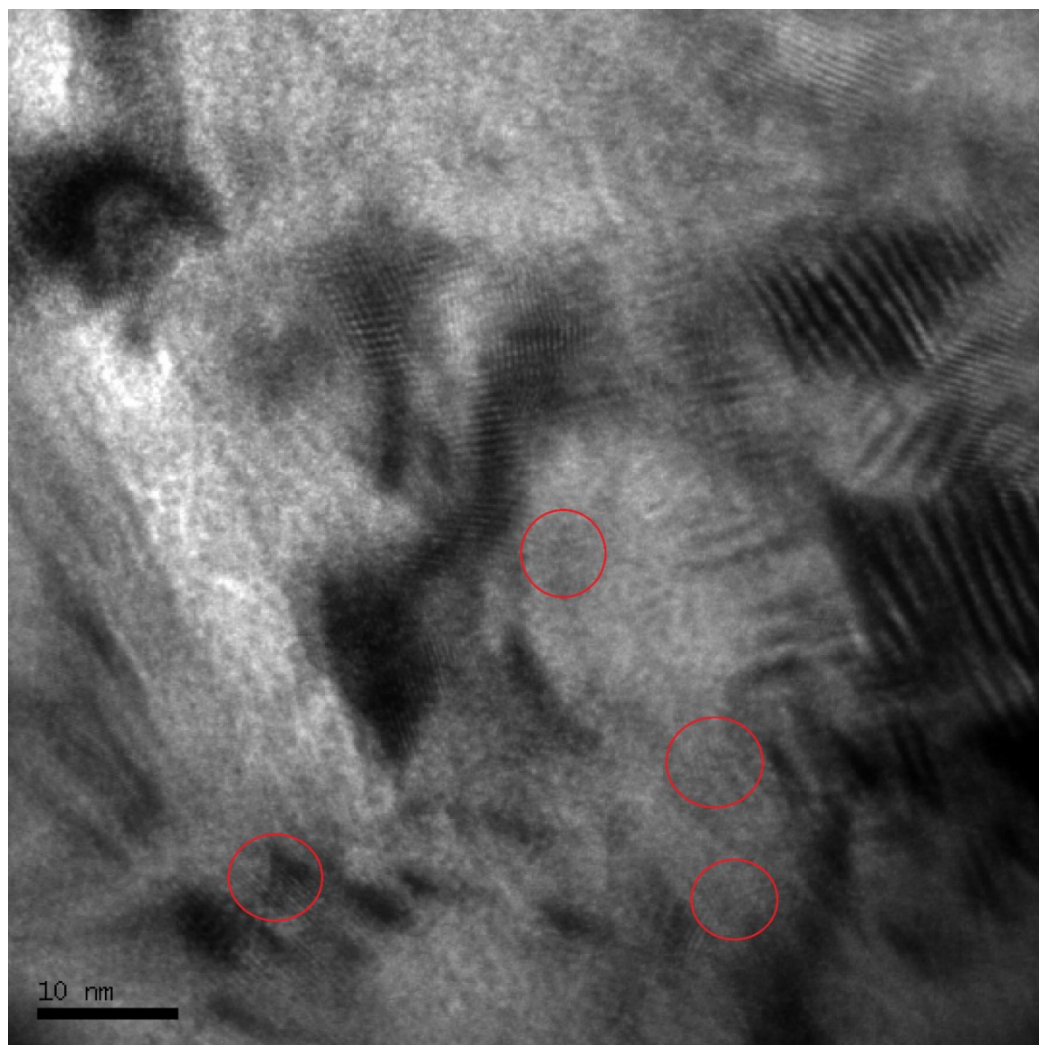


Figure S1. TEM image of NP1 material. Single particles in anatase 101 orientation (inter fringe distance 0.35 nm displaying particles are encircled in red).

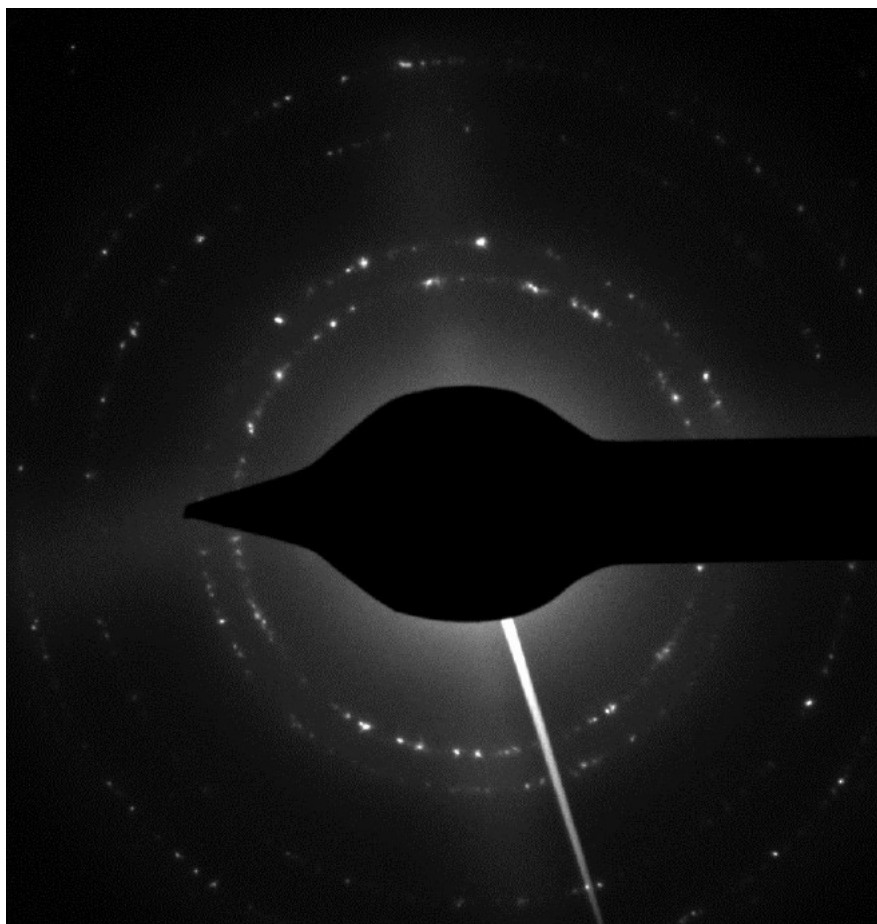


Figure S2. Selected area electron diffraction for anatase nanocrystals in NP1 material.

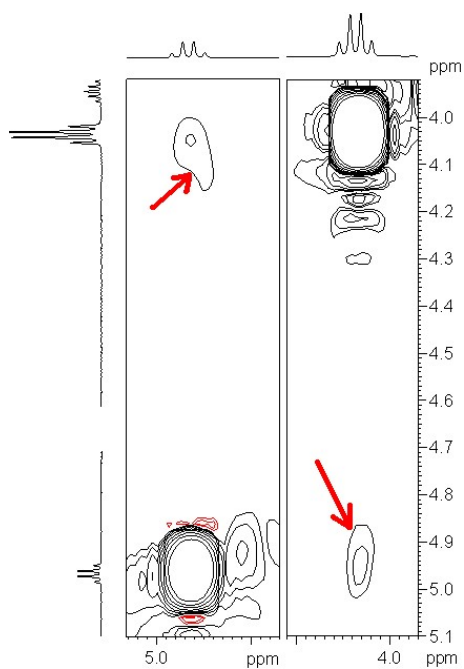


Figure S3. Fragment of NOESY spectrum of diluted TiBALDH in the lactate *CH* region showing correlations signals (indicated by red arrows) for the ligand exchange between $[\text{Ti}(\text{Lactate})_3]^{2-}$, and oxo-lactate/lactate capped nano- TiO_2 and confirming chelated binding of the lactate ligand to titania NP (NP1).

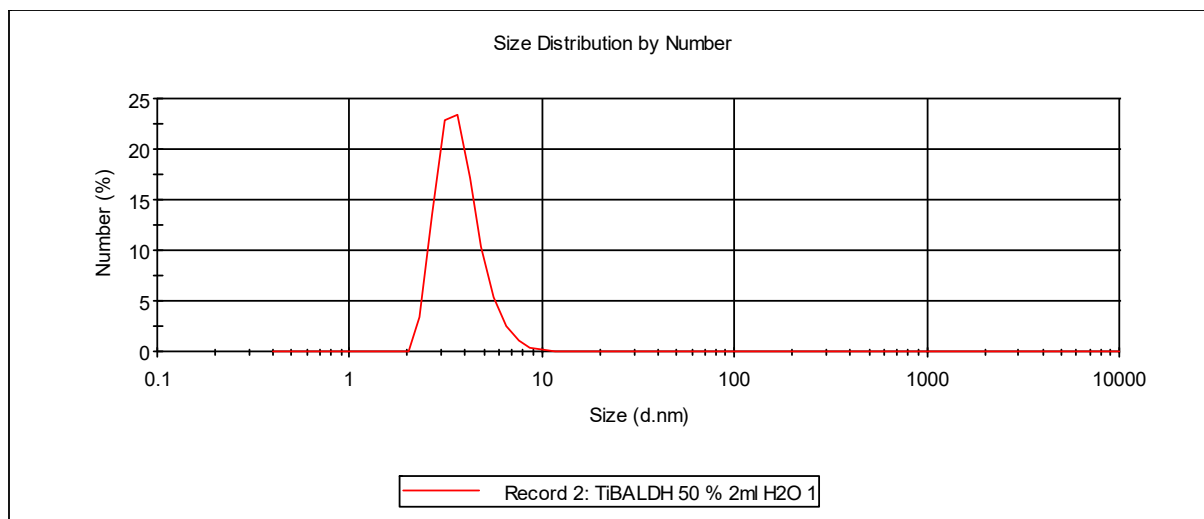


Figure S4. Hydrodynamic size distribution of the NP1 by DLS (Malvern instrument).

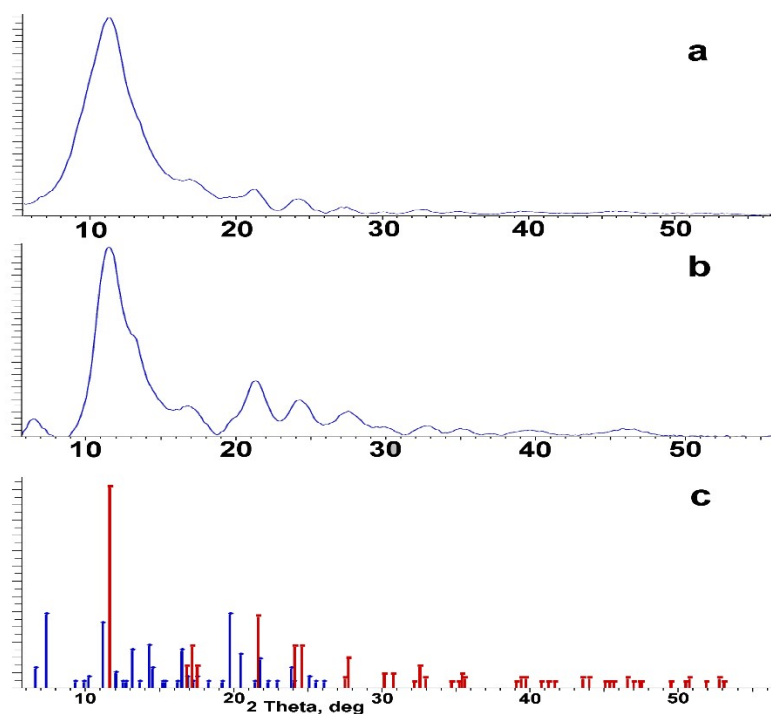


Figure S5. XRD of TiO₂ precipitated from TiBALDH by ethanol (NP1, a), 25% NH₃ (b) and the reference patterns of anatase, red, and H₂TiO₃, blue (c).

Biocompatibility of NP1 material

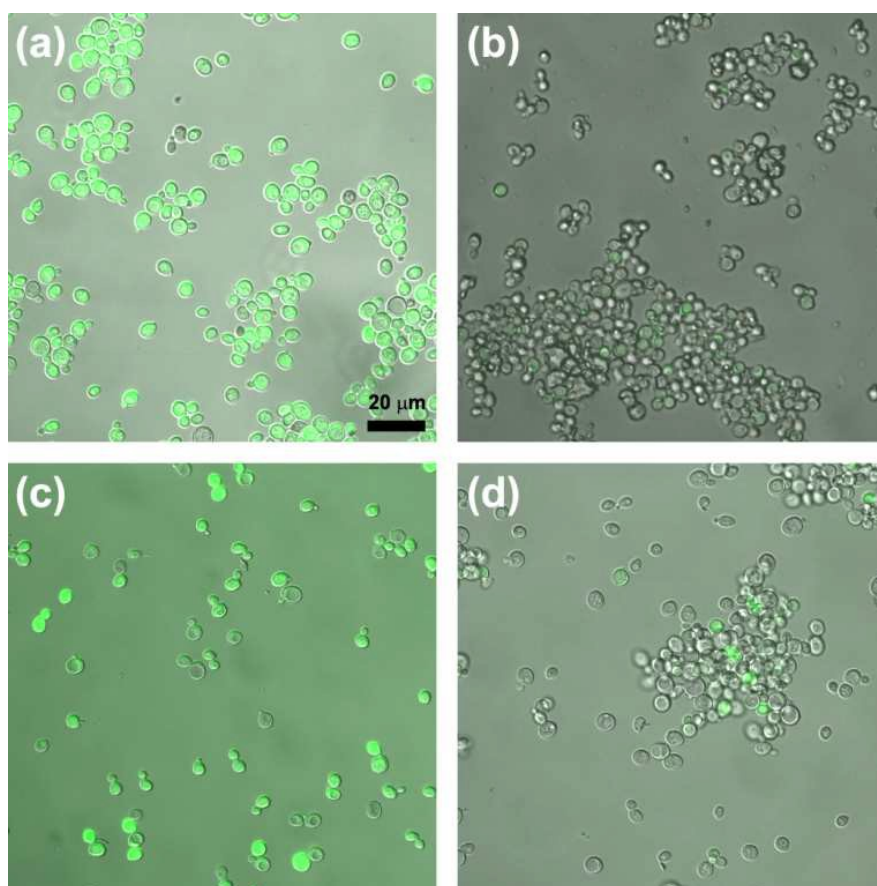


Figure S6. Viability test of (a) native yeast, (b) yeast@TiO₂, (c) native yeast with (RKK)4D8, and (d) native yeast with TBALDH. *Chlorella sp.* cells in green were considered alive, and the other ones were considered dead. The scale bar is 20 μm. Reproduced with permission from S.H. Yang, E.H. Ko, I.S. Choi, *Langmuir*, **2012**, 28, 4, 2151–2155.

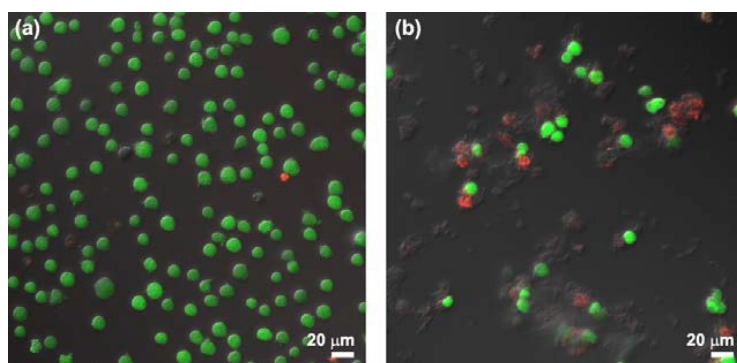


Figure S7. CLSM images of (a) native Jurkat cells and (b) Jurkat@TiO₂ (after 3 cycles in RPMI 1640 medium only). The LIVE/DEAD[®] viability/cytotoxicity kit was used for viability test. Green: alive; red: dead. Reproduced with permission from W. Youn, E.H. Ko, M.H. Kim, M. Park, D. Hong, G.A. Seisenbaeva, V.G. Kessler, I.S. Choi, *Angew. Chem. Int. Ed.*, **2017**, 56, 10702-10706.

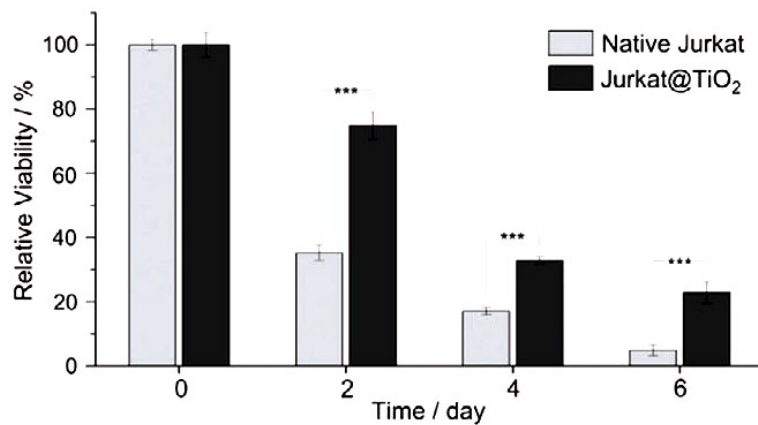


Figure S8. Cell viability of Jurkat cells with or without mineralized TiO₂ shells after incubation in serum-free culture media of 40°. Reproduced with permission from C.H. Lee, N. Kim, H.B. Rheem, B.J. Kim, J.H. Park, I.S. Choi, *Adv. Healthcare Mater.*, **2021**, 10, 2100347.

Description of NP2 material

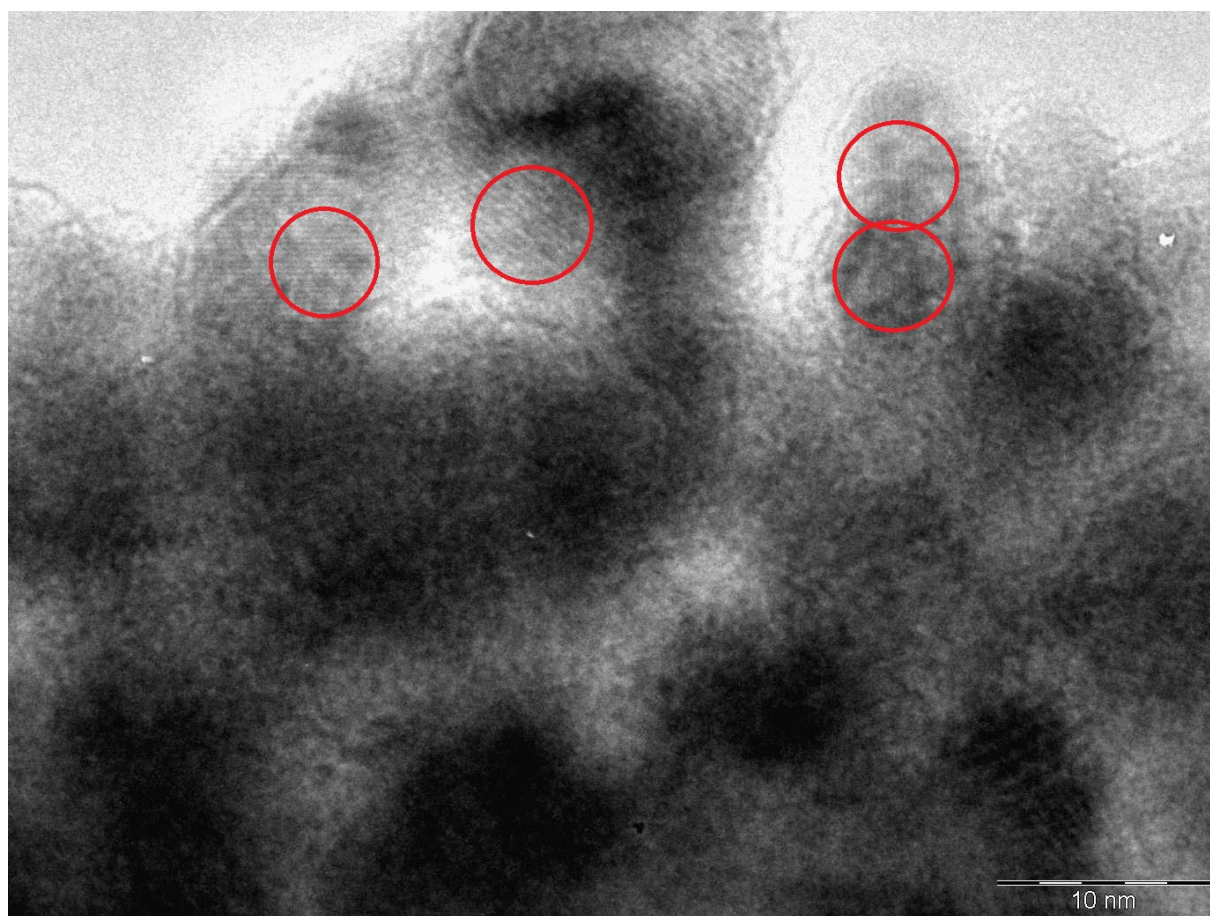


Figure S9. TEM image of NP2 material. Single particles in anatase 101 orientation (inter fringe distance 0.35 nm displaying particles are encircled in red). Reproduced with permission from Kessler V.G., Seisenbaeva G.A., Håkansson S., Unell M., *Chemically triggered biodelivery using metal-organic sol-gel synthesis*, *Angew. Chem.*, 2008, 47(44), 8506-8509.

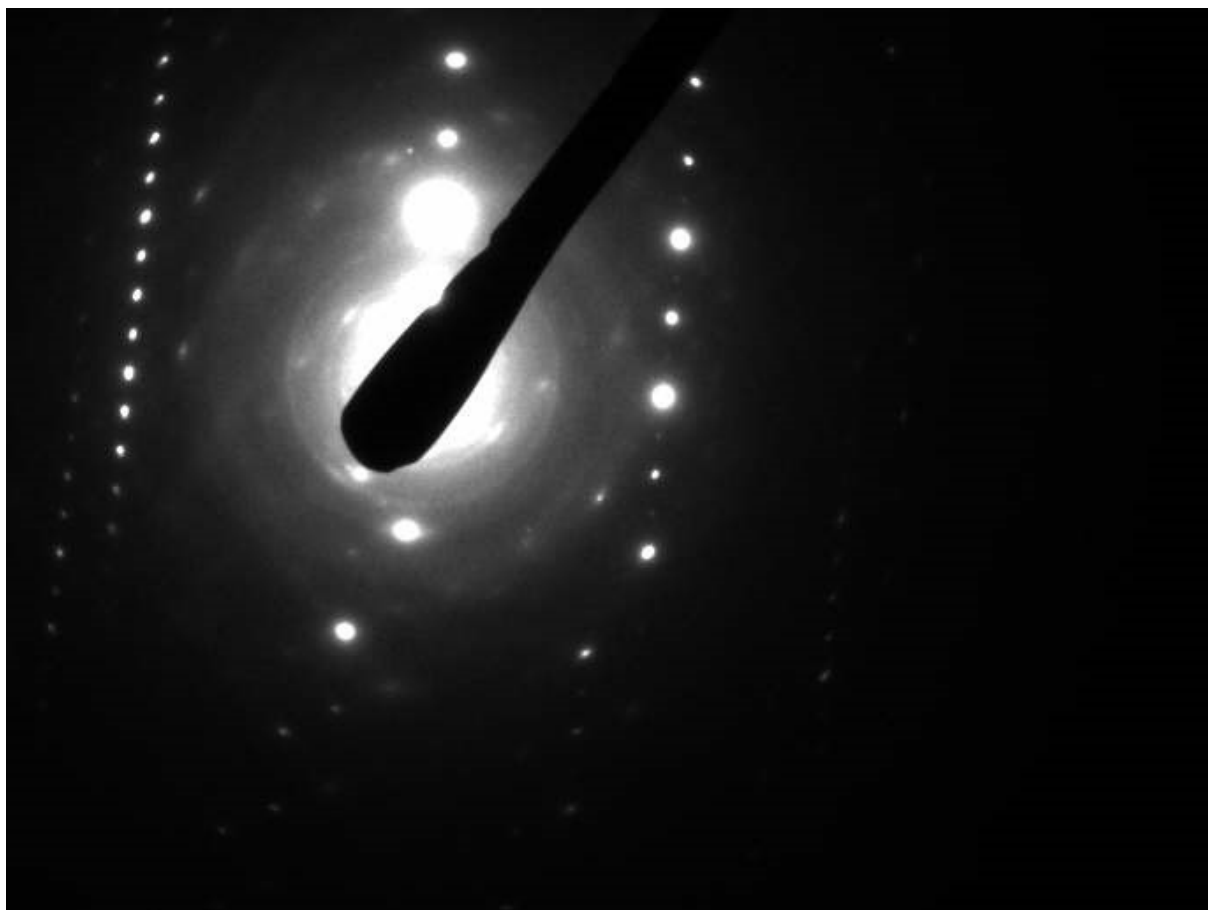


Figure S10. Selected area electron diffraction on a single crystallite of NP2, identifying it as anatase phase. Reproduced with permission from Kessler V.G., Seisenbaeva G.A., Håkansson S., Unell M., *Chemically triggered biodelivery using metal-organic sol-gel synthesis*, *Angew. Chem.*, 2008, 47(44), 8506-8509.

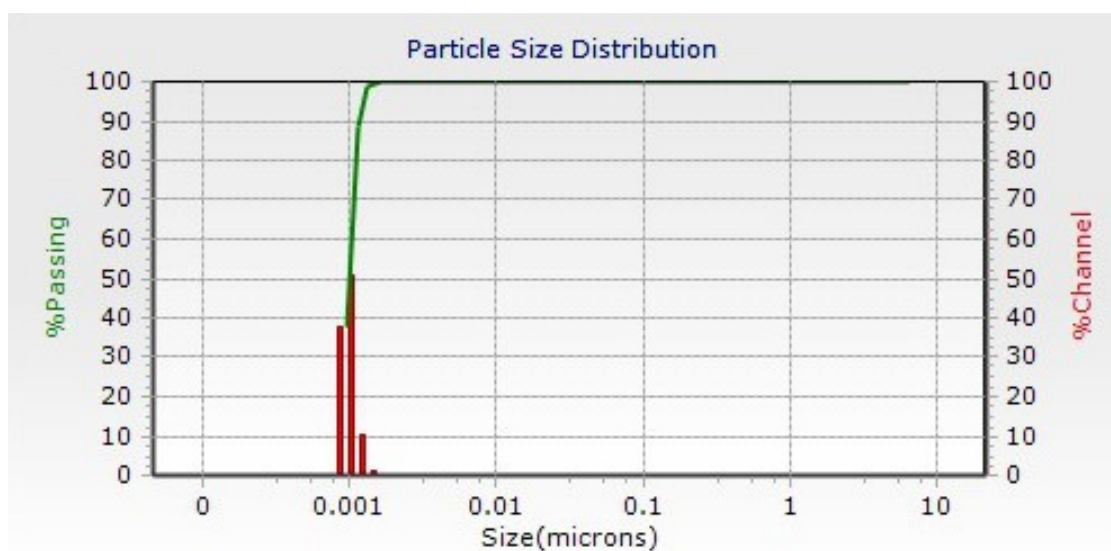
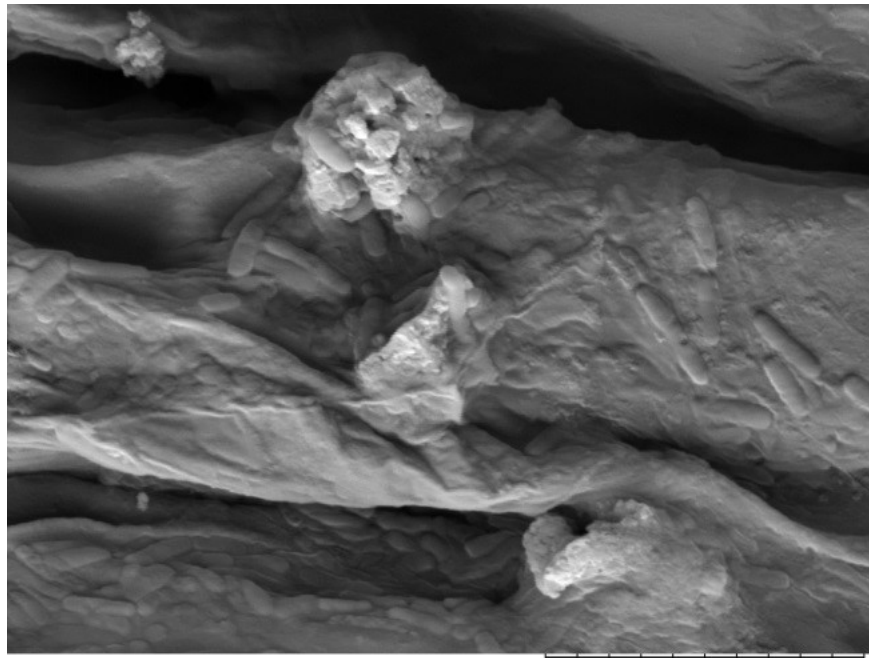


Figure S11. Hydrodynamic size distribution for NP2 by DLS (Microtrack instrument). Reproduced with permission from supplementary materials to Kessler V.G., Seisenbaeva G.A., Håkansson S., Unell M., *Chemically triggered biodelivery using metal-organic sol-gel synthesis*, *Angew. Chem.*, 2008, 47(44), 8506-8509.



TM-1000_0876 2011/07/27 15:56 L D2.7 x7.0k 10 um

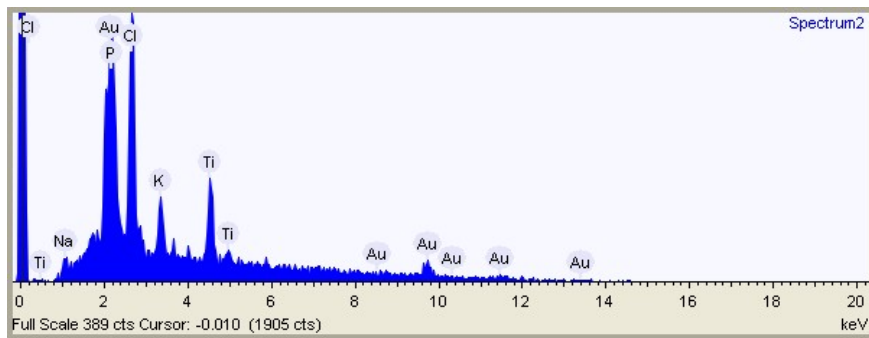


Figure S12. SEM view of *Bacillus amiloliquifasciens* bacteria artificial biofilm on roots of *Brassica napus* created by adding NP2 solution to bacterial culture for root treatment. Earlier unpublished image associated with the work by Palmqvist N. G. M., Bejai S., Meijer J., Seisenbaeva G. A., Kessler V. G., *Nano titania aided clustering and adhesion of beneficial bacteria to plant roots to enhance crop growth and stress management*, *Sci. Rep.* **2015**, 5, 10146. The sample was covered by gold to improve the resolution.

Biocompatibility of NP2

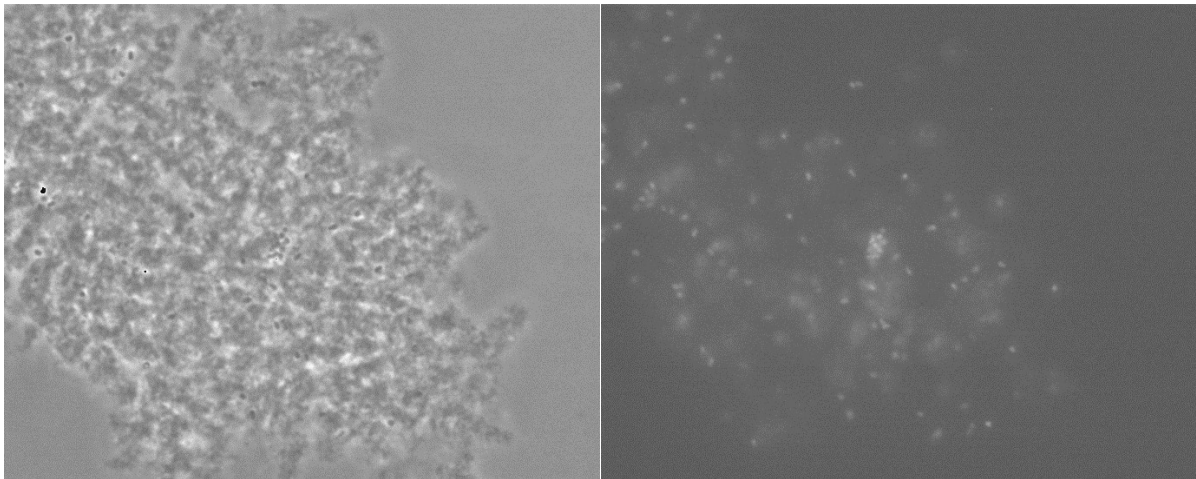


Figure S13. Viability of *A. chlorophenolicus* bacteria in encapsulation with NP2 material. Light optical microscopy image (left) and dark image (right). Luminescence indicates viable cells. Earlier unpublished image associated with the work by Kessler V.G., Seisenbaeva G.A., Håkansson S., Unell M., Chemically triggered biodelivery using metal-organic sol-gel synthesis, *Angew. Chem.*, 2008, 47(44), 8506-8509.

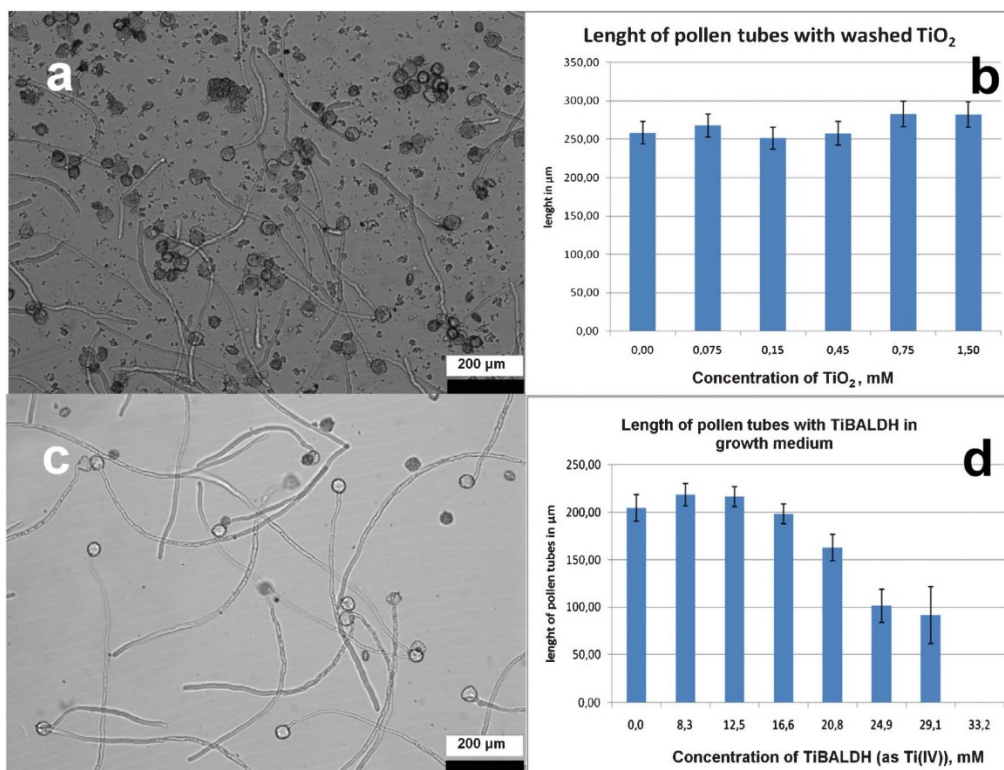


Figure S14. Growth of pollen tubes in a 100 mg ml⁻¹ suspension of titania gel produced from NP2 after 3 h of exposure (a). Length of pollen tubes measured in solutions with different concentrations of NP2 titania gel (b). Growth of pollen tubes in a 600 mg ml⁻¹ solution of NP1 (c). Length of pollen tubes measured in solutions with different concentrations of NP1 (d). Reproduced with permission from Groenke N., Seisenbaeva G.A., Kaminsky V., Zhivotovsky B., Kost B., Kessler V.G., Potential human health and environmental effects of the nano-titania-based bioencapsulation matrix and the model product of its biodegradation TiBALDH, *RSC Advances*, 2012, 2, 4228-4235.

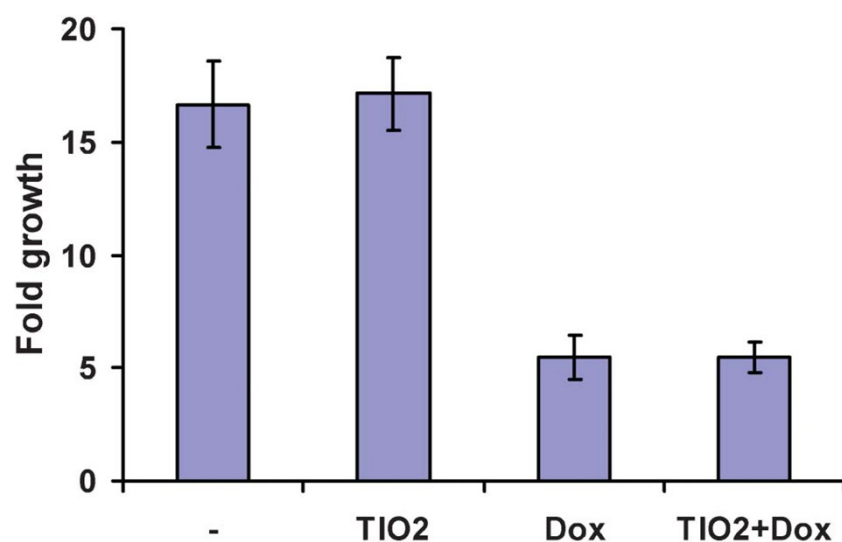


Figure S15. Growth of the cells treated with titanium oxide NP2 (50 mg ml⁻¹), doxorubicin (0.5 mg ml⁻¹) or their combination. Reproduced with permission from Groenke N., Seisenbaeva G.A., Kaminsky V., Zhivotovsky B., Kost B., Kessler V.G., Potential human health and environmental effects of the nano-titania-based bioencapsulation matrix and the model product of its biodegradation TiBALDH, RSC Advances, 2012, 2, 4228-4235.

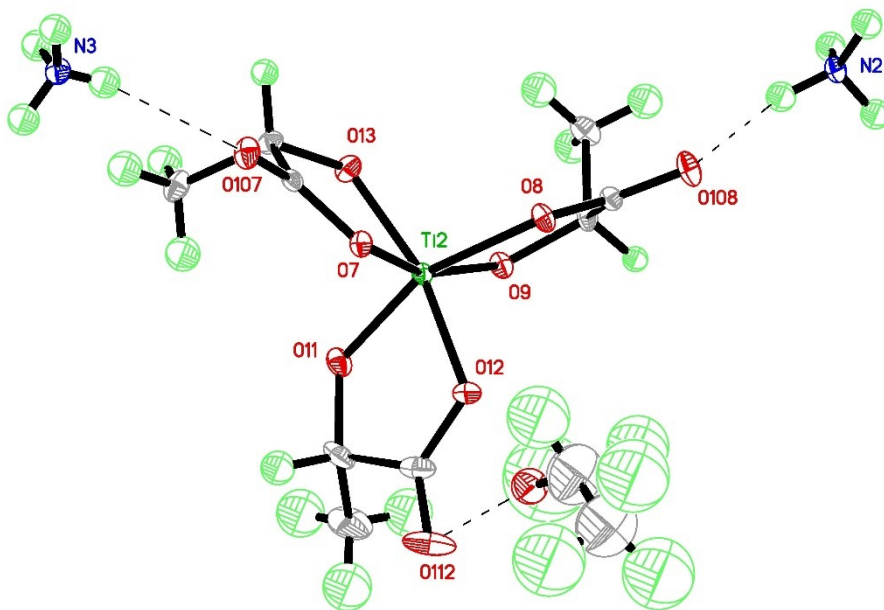


Figure S16. Fragment of the structure of $[(\text{NH}_4)_2\text{Ti}(\text{OCOCHOCH}_3)_3]_2 \cdot \text{EtOH}(\mathbf{1})$.

Table S1. Crystal data and structure refinement for (NH₄)₂Ti(Lact)₃.

Identification code	tio2et_test_210506_0m	
Empirical formula	C ₂₀ H ₅₀ N ₄ O ₁₅ Ti ₂	
Formula weight	682.44	
Temperature	296(2) K	
Wavelength	0.71073 Å	
Crystal system	Monoclinic	
Space group	C2	
Unit cell dimensions	a = 15.053(9) Å	α = 90°.
	b = 8.727(5) Å	β = 91.475(10)°.
	c = 25.957(15) Å	γ = 90°.
Volume	3409(3) Å ³	
Z	4	
Density (calculated)	1.330 Mg/m ³	
Absorption coefficient	0.534 mm ⁻¹	
F(000)	1448	
Crystal size	0.38 x 0.18 x 0.16 mm ³	
Theta range for data collection	2.71 to 25.02°.	
Index ranges	-17 ≤ h ≤ 17, -10 ≤ k ≤ 10, -30 ≤ l ≤ 30	
Reflections collected	14111	
Independent reflections	5760 [R(int) = 0.0346]	
Completeness to theta = 25.02°	97.0 %	
Absorption correction	Empirical	
Refinement method	Full-matrix least-squares on F ²	
Data / restraints / parameters	5760 / 344 / 426	
Goodness-of-fit on F ²	0.988	
Final R indices [I > 2σ(I)]	R1 = 0.0362, wR2 = 0.0833	
R indices (all data)	R1 = 0.0464, wR2 = 0.0951	
Absolute structure parameter	0.03(3)	
Largest diff. peak and hole	0.612 and -0.477 e.Å ⁻³	

Table S2. Atomic coordinates ($\times 10^4$) and equivalent isotropic displacement parameters ($\text{\AA}^2 \times 10^3$) for $(\text{NH}_4)_2\text{Ti}(\text{Lact})_3$. $U(\text{eq})$ is defined as one third of the trace of the orthogonalized U^{ij} tensor.

	x	y	z	$U(\text{eq})$
Ti(1)	1706(1)	5067(1)	1275(1)	27(1)
O(1)	1157(2)	3416(3)	1612(1)	36(1)
O(2)	2759(2)	4977(3)	1679(1)	36(1)
O(3)	1177(2)	6653(3)	1633(1)	38(1)
O(4)	1897(2)	6861(3)	785(1)	44(1)
O(5)	748(2)	4485(3)	749(1)	43(1)
O(102)	-451(2)	3060(6)	626(1)	92(1)
O(105)	3913(2)	3106(6)	698(1)	81(1)
O(6)	2536(2)	3979(3)	785(1)	42(1)
O(10)	1653(3)	9363(4)	669(2)	87(1)
C(1)	337(2)	2841(5)	1422(2)	43(1)
C(11)	-414(3)	3243(7)	1770(2)	65(2)
C(4)	1181(3)	8177(5)	1446(2)	44(1)
C(41)	1642(4)	9255(6)	1817(2)	74(2)
C(6)	3506(2)	4148(5)	1508(2)	38(1)
C(5)	3338(3)	3705(5)	948(2)	44(1)
C(2)	171(3)	3458(5)	887(2)	46(1)
C(61)	3693(3)	2737(7)	1842(2)	64(1)
Ti(2)	4036(1)	2821(1)	3729(1)	36(1)
C(8)	5452(3)	4998(6)	3717(2)	45(1)
O(7)	3259(2)	1718(3)	3182(1)	44(1)
O(8)	4323(2)	4256(4)	3129(1)	49(1)
O(9)	4955(2)	3992(4)	4019(1)	48(1)
O(11)	3550(2)	2129(4)	4338(1)	59(1)
O(12)	2953(2)	4189(4)	3763(1)	60(1)
C(7)	4976(3)	5175(6)	3199(2)	44(1)
O(108)	5196(2)	6129(4)	2885(1)	68(1)
C(9)	3486(3)	325(5)	3072(2)	41(1)
O(107)	3093(2)	-471(4)	2754(1)	61(1)
O(13)	4699(2)	1062(4)	3602(1)	53(1)
C(81)	6386(3)	4449(7)	3659(2)	69(2)
C(10)	4280(3)	-249(5)	3377(2)	49(1)
O(112)	1710(3)	4543(8)	4165(2)	135(2)

C(12)	2737(4)	2700(9)	4499(2)	79(2)
C(101)	3975(4)	-1382(6)	3790(2)	66(1)
N(4)	5000	1530(5)	0	38(1)
N(1)	-1834(2)	1923(4)	-13(1)	40(1)
N(2)	6678(2)	7770(5)	2633(1)	49(1)
C(3)	1603(3)	8189(5)	924(2)	46(1)
N(3)	2962(3)	-3665(4)	2643(1)	50(1)
C(21)	2424(4)	3918(8)	4123(2)	76(2)
C(121)	2803(6)	3293(12)	5049(3)	133(3)
O(5A)	5000	5353(9)	5000	112(2)
O(6A)	1424(3)	5558(6)	3214(2)	103(2)
O(7A)	4610(5)	926(11)	5174(3)	84(2)
O(8A)	5447(5)	-1613(11)	4874(3)	89(3)
C(2A)	358(10)	6740(20)	2524(6)	251(7)
C(1A)	1121(10)	6090(20)	2783(5)	244(7)

Table S3. Bond lengths [\AA] and angles [$^\circ$] for $(\text{NH}_4)_2\text{Ti}(\text{Lact})_3$.

Ti(1)-O(3)	1.857(3)
Ti(1)-O(2)	1.879(2)
Ti(1)-O(1)	1.887(3)
Ti(1)-O(5)	2.025(3)
Ti(1)-O(6)	2.040(3)
Ti(1)-O(4)	2.043(3)
O(1)-C(1)	1.411(5)
O(2)-C(6)	1.419(4)
O(3)-C(4)	1.416(5)
O(4)-C(3)	1.296(5)
O(5)-C(2)	1.305(5)
O(102)-C(2)	1.194(5)
O(105)-C(5)	1.214(5)
O(6)-C(5)	1.291(5)
O(10)-C(3)	1.222(5)
C(1)-C(2)	1.503(6)
C(1)-C(11)	1.506(6)
C(1)-H(1)	0.9800
C(11)-H(11A)	0.9600
C(11)-H(11B)	0.9600
C(11)-H(11C)	0.9600
C(4)-C(41)	1.504(6)
C(4)-C(3)	1.512(6)
C(4)-H(4)	0.9800
C(41)-H(41A)	0.9600
C(41)-H(41B)	0.9600
C(41)-H(41C)	0.9600
C(6)-C(5)	1.519(6)
C(6)-C(61)	1.527(6)
C(6)-H(6)	0.9800
C(61)-H(61A)	0.9600
C(61)-H(61B)	0.9600
C(61)-H(61C)	0.9600
Ti(2)-O(11)	1.860(3)
Ti(2)-O(9)	1.863(3)
Ti(2)-O(13)	1.865(3)

Ti(2)-O(12)	2.024(3)
Ti(2)-O(8)	2.053(3)
Ti(2)-O(7)	2.055(3)
C(8)-O(9)	1.406(5)
C(8)-C(81)	1.497(6)
C(8)-C(7)	1.516(6)
C(8)-H(8)	0.9800
O(7)-C(9)	1.297(5)
O(8)-C(7)	1.278(5)
O(11)-C(12)	1.396(7)
O(12)-C(21)	1.267(6)
C(7)-O(108)	1.216(5)
C(9)-O(107)	1.218(5)
C(9)-C(10)	1.504(6)
O(13)-C(10)	1.425(5)
C(81)-H(81A)	0.9600
C(81)-H(81B)	0.9600
C(81)-H(81C)	0.9600
C(10)-C(101)	1.538(7)
C(10)-H(10)	0.9800
O(112)-C(21)	1.214(7)
C(12)-C(21)	1.510(9)
C(12)-C(121)	1.518(9)
C(12)-H(12)	0.9800
C(101)-H(10A)	0.9600
C(101)-H(10B)	0.9600
C(101)-H(10C)	0.9600
N(4)-H(41A)	1.0184
N(4)-H(42A)	0.9134
N(1)-H(11A)	0.9225
N(1)-H(12A)	0.7376
N(1)-H(13A)	0.8041
N(1)-H(14A)	0.9104
N(2)-H(21A)	0.8955
N(2)-H(22A)	1.1037
N(2)-H(23A)	0.9173
N(2)-H(24A)	0.9075
N(3)-H(31A)	0.8881

N(3)-H(32A)	0.8105
N(3)-H(33A)	0.6551
N(3)-H(34A)	0.8892
C(121)-H(12A)	0.9600
C(121)-H(12B)	0.9600
C(121)-H(12C)	0.9600
O(5A)-H(5AA)	0.8498
O(6A)-C(1A)	1.285(8)
O(6A)-H(6AA)	1.1464
O(7A)-O(7A)#1	1.501(15)
O(8A)-O(8A)#1	1.511(15)
C(2A)-C(1A)	1.433(9)
C(2A)-H(2A1)	0.9600
C(2A)-H(2A2)	0.9600
C(2A)-H(2A3)	0.9600
C(1A)-H(1A1)	0.9700
C(1A)-H(1A2)	0.9700
O(3)-Ti(1)-O(2)	96.79(13)
O(3)-Ti(1)-O(1)	97.97(11)
O(2)-Ti(1)-O(1)	94.72(12)
O(3)-Ti(1)-O(5)	102.49(13)
O(2)-Ti(1)-O(5)	160.34(12)
O(1)-Ti(1)-O(5)	78.93(12)
O(3)-Ti(1)-O(6)	159.36(12)
O(2)-Ti(1)-O(6)	78.93(11)
O(1)-Ti(1)-O(6)	102.49(13)
O(5)-Ti(1)-O(6)	84.27(12)
O(3)-Ti(1)-O(4)	79.00(13)
O(2)-Ti(1)-O(4)	104.48(13)
O(1)-Ti(1)-O(4)	160.76(12)
O(5)-Ti(1)-O(4)	83.17(12)
O(6)-Ti(1)-O(4)	82.54(13)
C(1)-O(1)-Ti(1)	119.9(2)
C(6)-O(2)-Ti(1)	120.7(2)
C(4)-O(3)-Ti(1)	121.6(3)
C(3)-O(4)-Ti(1)	117.2(3)
C(2)-O(5)-Ti(1)	117.1(2)

C(5)-O(6)-Ti(1)	117.6(3)
O(1)-C(1)-C(2)	108.6(3)
O(1)-C(1)-C(11)	111.7(4)
C(2)-C(1)-C(11)	111.2(4)
O(1)-C(1)-H(1)	108.4
C(2)-C(1)-H(1)	108.4
C(11)-C(1)-H(1)	108.4
C(1)-C(11)-H(11A)	109.5
C(1)-C(11)-H(11B)	109.5
H(11A)-C(11)-H(11B)	109.5
C(1)-C(11)-H(11C)	109.5
H(11A)-C(11)-H(11C)	109.5
H(11B)-C(11)-H(11C)	109.5
O(3)-C(4)-C(41)	112.0(4)
O(3)-C(4)-C(3)	108.6(3)
C(41)-C(4)-C(3)	111.9(4)
O(3)-C(4)-H(4)	108.1
C(41)-C(4)-H(4)	108.1
C(3)-C(4)-H(4)	108.1
C(4)-C(41)-H(41A)	109.5
C(4)-C(41)-H(41B)	109.5
H(41A)-C(41)-H(41B)	109.5
C(4)-C(41)-H(41C)	109.5
H(41A)-C(41)-H(41C)	109.5
H(41B)-C(41)-H(41C)	109.5
O(2)-C(6)-C(5)	108.4(3)
O(2)-C(6)-C(61)	111.7(3)
C(5)-C(6)-C(61)	111.2(4)
O(2)-C(6)-H(6)	108.5
C(5)-C(6)-H(6)	108.5
C(61)-C(6)-H(6)	108.5
O(105)-C(5)-O(6)	125.2(4)
O(105)-C(5)-C(6)	121.2(4)
O(6)-C(5)-C(6)	113.5(3)
O(102)-C(2)-O(5)	124.2(4)
O(102)-C(2)-C(1)	122.0(4)
O(5)-C(2)-C(1)	113.8(3)
C(6)-C(61)-H(61A)	109.5

C(6)-C(61)-H(61B)	109.5
H(61A)-C(61)-H(61B)	109.5
C(6)-C(61)-H(61C)	109.5
H(61A)-C(61)-H(61C)	109.5
H(61B)-C(61)-H(61C)	109.5
O(11)-Ti(2)-O(9)	97.93(14)
O(11)-Ti(2)-O(13)	96.07(16)
O(9)-Ti(2)-O(13)	97.34(14)
O(11)-Ti(2)-O(12)	79.62(15)
O(9)-Ti(2)-O(12)	104.41(15)
O(13)-Ti(2)-O(12)	158.20(14)
O(11)-Ti(2)-O(8)	159.72(15)
O(9)-Ti(2)-O(8)	78.70(13)
O(13)-Ti(2)-O(8)	104.18(15)
O(12)-Ti(2)-O(8)	81.88(14)
O(11)-Ti(2)-O(7)	101.85(14)
O(9)-Ti(2)-O(7)	160.03(12)
O(13)-Ti(2)-O(7)	77.92(13)
O(12)-Ti(2)-O(7)	82.05(14)
O(8)-Ti(2)-O(7)	83.64(12)
O(9)-C(8)-C(81)	111.8(4)
O(9)-C(8)-C(7)	108.2(3)
C(81)-C(8)-C(7)	111.5(4)
O(9)-C(8)-H(8)	108.4
C(81)-C(8)-H(8)	108.4
C(7)-C(8)-H(8)	108.4
C(9)-O(7)-Ti(2)	116.3(3)
C(7)-O(8)-Ti(2)	116.8(3)
C(8)-O(9)-Ti(2)	121.1(2)
C(12)-O(11)-Ti(2)	120.4(4)
C(21)-O(12)-Ti(2)	116.4(4)
O(108)-C(7)-O(8)	123.9(4)
O(108)-C(7)-C(8)	122.2(4)
O(8)-C(7)-C(8)	114.0(4)
O(107)-C(9)-O(7)	123.9(4)
O(107)-C(9)-C(10)	122.1(4)
O(7)-C(9)-C(10)	114.0(3)
C(10)-O(13)-Ti(2)	120.0(3)

C(8)-C(81)-H(81A)	109.5
C(8)-C(81)-H(81B)	109.5
H(81A)-C(81)-H(81B)	109.5
C(8)-C(81)-H(81C)	109.5
H(81A)-C(81)-H(81C)	109.5
H(81B)-C(81)-H(81C)	109.5
O(13)-C(10)-C(9)	106.6(3)
O(13)-C(10)-C(101)	111.5(4)
C(9)-C(10)-C(101)	109.5(4)
O(13)-C(10)-H(10)	109.7
C(9)-C(10)-H(10)	109.7
C(101)-C(10)-H(10)	109.7
O(11)-C(12)-C(21)	108.6(4)
O(11)-C(12)-C(121)	111.6(6)
C(21)-C(12)-C(121)	112.3(7)
O(11)-C(12)-H(12)	108.1
C(21)-C(12)-H(12)	108.1
C(121)-C(12)-H(12)	108.1
C(10)-C(101)-H(10A)	109.5
C(10)-C(101)-H(10B)	109.5
H(10A)-C(101)-H(10B)	109.5
C(10)-C(101)-H(10C)	109.5
H(10A)-C(101)-H(10C)	109.5
H(10B)-C(101)-H(10C)	109.5
H(41A)-N(4)-H(42A)	111.2
H(11A)-N(1)-H(12A)	103.2
H(11A)-N(1)-H(13A)	114.1
H(12A)-N(1)-H(13A)	107.1
H(11A)-N(1)-H(14A)	105.5
H(12A)-N(1)-H(14A)	103.8
H(13A)-N(1)-H(14A)	121.3
H(21A)-N(2)-H(22A)	113.2
H(21A)-N(2)-H(23A)	109.5
H(22A)-N(2)-H(23A)	119.7
H(21A)-N(2)-H(24A)	109.2
H(22A)-N(2)-H(24A)	113.7
H(23A)-N(2)-H(24A)	89.0
O(10)-C(3)-O(4)	125.0(4)

O(10)-C(3)-C(4)	121.6(4)
O(4)-C(3)-C(4)	113.5(3)
H(31A)-N(3)-H(32A)	111.1
H(31A)-N(3)-H(33A)	107.3
H(32A)-N(3)-H(33A)	112.8
H(31A)-N(3)-H(34A)	114.6
H(32A)-N(3)-H(34A)	105.5
H(33A)-N(3)-H(34A)	105.6
O(112)-C(21)-O(12)	123.8(7)
O(112)-C(21)-C(12)	121.4(6)
O(12)-C(21)-C(12)	114.7(5)
C(12)-C(121)-H(12A)	109.5
C(12)-C(121)-H(12B)	109.5
H(12A)-C(121)-H(12B)	109.5
C(12)-C(121)-H(12C)	109.5
H(12A)-C(121)-H(12C)	109.5
H(12B)-C(121)-H(12C)	109.5
C(1A)-O(6A)-H(6AA)	137.7
C(1A)-C(2A)-H(2A1)	109.5
C(1A)-C(2A)-H(2A2)	109.5
H(2A1)-C(2A)-H(2A2)	109.5
C(1A)-C(2A)-H(2A3)	109.5
H(2A1)-C(2A)-H(2A3)	109.5
H(2A2)-C(2A)-H(2A3)	109.5
O(6A)-C(1A)-C(2A)	144.4(14)
O(6A)-C(1A)-H(1A1)	100.8
C(2A)-C(1A)-H(1A1)	100.8
O(6A)-C(1A)-H(1A2)	100.8
C(2A)-C(1A)-H(1A2)	100.8
H(1A1)-C(1A)-H(1A2)	104.4

Symmetry transformations used to generate equivalent atoms:

#1 -x+1,y,-z+1